Rapid Temporal Control of Transdermal Drug Delivery by Electroporation

Mark R. Prausnitz,[1,2] Uwe Pliquett,[3] Robert Langer,[1,3,4] and James C. Weaver[3,4]

Received May 5, 1994; accepted July 1, 1994

KEY WORDS: transdermal drug delivery; electroporation; iontophoresis; human skin; percutaneous transport; flow-through system.

INTRODUCTION

Transdermal drug delivery has the potential to be a noninvasive, user-friendly method of delivering drugs at steady or time-varying rates (1,2). However, to date it has found limited clinical application, largely because transport of most drugs across human skin is very slow, exhibiting lag times of hours to days and steady-state rates which are often subtherapeutic. Recently, evidence for electroporation of skin has been demonstrated and proposed as a mechanism to enhance transdermal drug delivery (3–7).

Electroporation involves the application of a brief electric field pulse which creates aqueous pathways in lipid bilayers, such as cell membranes (8–11). During electroporation, the electric field is believed to increase molecular transport dramatically by a combination of two mechanisms: 1) electropores are created and 2) as pores appear, molecules are rapidly moved through the pores by electrophoresis and/or electroosmosis due to the local field.

Electroporation of skin could have significance for drug delivery, having been shown to cause transdermal flux increases up to four orders of magnitude which are largely or fully reversible, possibly involving transient structural changes in the intercellular lipid bilayers of the stratum corneum (5,12). This study focuses on the rapid kinetics of transdermal transport by electroporation, which may allow rapid onset of therapeutic action and/or complex drug delivery profiles during transdermal drug delivery.

MATERIALS AND METHODS

The experimental methods have been described previously (5,13). Briefly, heat stripped human epidermis was loaded into a side-by-side, flow-through permeation chamber containing well-stirred phosphate-buffered saline (PBS; pH 7.4, 150 mM total salts; Sigma, St. Louis, MO) at 21 ± 3°C. A donor solution of 1 mM calcein (Sigma) in PBS was placed in the donor compartment, facing the stratum corneum (0.7 cm^2 exposed skin). Contents of the receptor compartment (facing the viable epidermis) were continuously flowed through a spectrofluorimeter ($\lambda_{excitation}$ = 488 nm, $\lambda_{emission}$ = 515 nm; Fluorolog-2, model F112AI, SPEX Industries, Edison, NJ) allowing continuous determination of receptor solution fluorescence. Deconvolution and calibration of the fluorescence measurements allowed calculation of transdermal fluxes with 20 s resolution (13).

After allowing skin to hydrate for 1–2 h, electric field pulses (exponential-decay time constant, τ = 1.1 msec) were applied with an Electro Cell Manipulator 600 (BTX, San Diego, CA) using Ag/AgCl electrodes (In Vivo Metrics, Healdsburg, CA), each located 3 cm from the skin. Iontophoresis was performed with a constant-current power supply. The negative electrode was in the donor compartment, while the positive electrode was in the receptor compartment. Reported voltages are average transdermal values, determined ~10 μs after the onset of each pulse. Because significant voltage drops occurred within donor and receptor solutions, applied voltages were significantly higher (5,6,14).

RESULTS

Transdermal transport by electroporation of calcein across human epidermis was continuously measured (Figure 1). Figure 1A shows calcein flux versus time due to pulsing at three different voltages at the same pulse rate (1 pulse per minute, ppm) for 1 h. At each voltage, flux reached a steady state within minutes and then decreased below background levels within seconds after pulsing stopped. Passive transport of calcein was below the detection limit (on the order of 1 ng/cm^2h).

At first, the curves in Figure 1A may appear to contain a lot of noise. However, the same data shown with an expanded time axis in Figure 1B, indicates that flux varied with a regular period of approximately 1 peak per minute. This is the same rate at which pulses were applied. Our interpretation is that these variations show the effects on transport of individual pulses. This is also supported by results seen during pulsing at other rates (data not shown). After each pulse, the flux initially increased, but then decayed as the effects of the pulse decreased. Although the time over which the flux decayed after each pulse appears to be tens of seconds, it may be shorter, as discussed previously (13).

Figure 1C shows this data replotted as cumulative calcein transported. From the graph, steady-state lag times (the characteristic time for flux to reach steady state) can be calculated by extending the linear portion of the graph to the time axis. The intercept is the steady-state lag time, determined to be approximately 10 min, independent of voltage. Figure 1D, which shows the same data with an expanded time axis, indicates that the onset time for transport was 3 min, independent of voltage: pulsing was started at 3 min and the first detectable transdermal transport was measured at 6 min.

Data similar to that of Figure 1 have been collected over a range of pulsing conditions. Characteristic values describ-

[1] Department of Chemical Engineering, Massachusetts Institute of Technology, Cambridge, Massachusetts 02139.

[2] Present address: School of Chemical Engineering, Georgia Institute of Technology, Atlanta, Georgia 30332.

[3] Harvard-MIT Division of Health Sciences and Technology, Massachusetts Institute of Technology, Cambridge, Massachusetts 02139.

[4] To whom correspondence should be addressed.

0724-8741/94/1200-1834$07.00/0

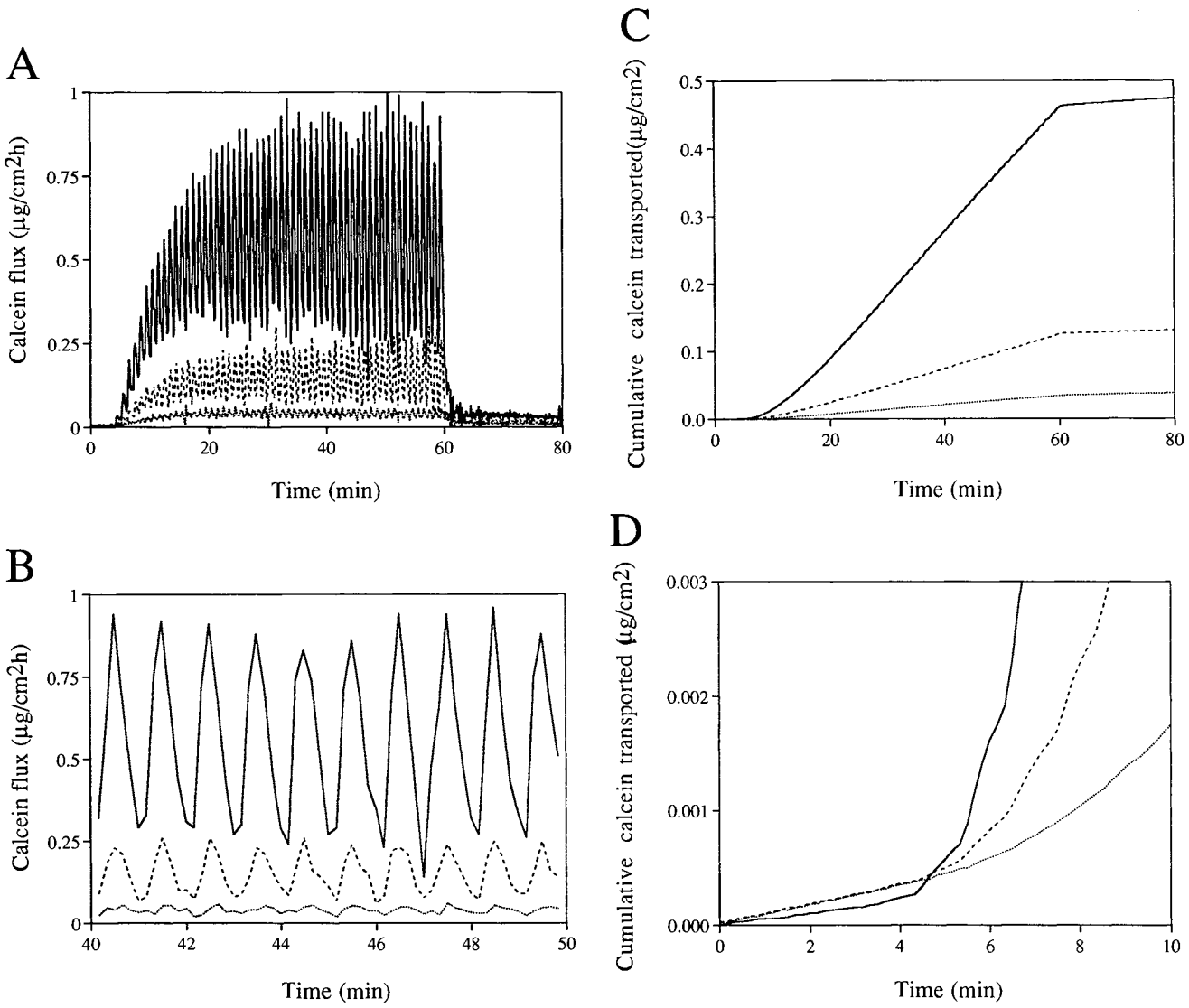

Fig. 1. Time profiles of transdermal transport of calcein due to electroporation at different voltages. A) Transdermal flux due to pulsing at 1 pulse per minute (ppm) for 1 h: 270 V (solid line), 135 V (dashed line), 115 V (dotted line). B) Data in (A) with the time axis expanded. C) Data in (A) replotted as cumulative calcein transported, for calculation of steady-state lag times, indicated by the time-axis intercept. D) Data in (C) with the time axis expanded, to show transport onset time. The data in this figure are representative of results seen in >20 similar experiments. These graphs demonstrate that transdermal flux was rapidly responsive to electrical conditions, over characteristic times of seconds to minutes (see Table I).

ing these data are summarized in Table I. They indicate that while flux depended on both pulse voltage and pulse rate, the steady-state lag time and onset time depended only on pulse rate. Decay time was independent of both pulse voltage and pulse rate.

Using the data in Table I, flux as a function of time was empirically fit by the following equations:

$$J = J_{ss}\left[1 - e^{\frac{-(t - T)}{\tau}}\right] \quad (1)$$

$$J_{ss} = k_1 V R \quad (2)$$

$$\tau = \frac{k_2}{R} \quad (3)$$

$$T = \frac{k_3}{R} \quad (4)$$

where J = calcein flux ($\mu g/cm^2h$), J_{SS} = steady-state calcein flux ($\mu g/cm^2h$), t = time (min), T = onset time (min), τ = steady-state lag time (min), V = pulse voltage (V), R = pulse rate (ppm), and k_1, k_2, and k_3, are empirical constants equal to 8×10^{-4} $\mu g/(cm^2hVppm)$, 10, and 4 respectively.

The three empirical constants were determined using the data in Table I. To calculate k_1, steady-state flux was plotted versus the product of pulse voltage time pulse rate and a least-squares linear regression was performed (r^2 = 0.83) yielding a slope equal to k_1. Similarly, k_2 equalled the slope of a linear fit of steady-state lag time versus the inverse of pulse rate (r^2 = 0.95). Average onset time corresponded to

Table I. Characteristic Values of Transdermal Transport of Calcein Due to Electroporation[a]

Pulse conditions			
Pulse voltage (V)	Pulse rate (ppm)	Steady-state flux ($\mu g/cm^2hr$)	Steady-state lag time (min)[bcd]
63	1	0.055	13
63	3	0.074	
63	6	0.11	
63	12	0.14	
86	1	0.073	10
86	3	0.13	
86	6	0.25	
86	12	0.49	
134	1	0.16	12
134	3	0.30	
134	6	0.47	
134	12	0.74	
191	1	0.1	11
191	3	0.43	5
191	6	1.1	3
191	12	2.1	2
231	1	0.24	11
231	3	0.64	6
231	6		1
231	12		1

[a] Each data point is the average of 1–2 experimental values, including results from a total of 15 different skin samples.
[b] Steady-state lag time (the characteristic time for flux to reach steady state) corresponds to the time-axis intercept of graphs of cumulative calcein transported vs time (see Fig. 1C).
[c] Onset time, which indicates the time at which an increased flux was first measured (see Fig 1D), generally corresponded to the time required to give 3–5 pulses (e.g., 3–5 min for 1 ppm or 15–25 s for 12 ppm). Onset detection limit was on the order of 1 $ng/cm^2/h$.
[d] Decay time, which corresponds to the characteristic time over which flux decayed after pulsing was stopped, was <10 s under all conditions investigated (determined by fitting to an exponential decay).

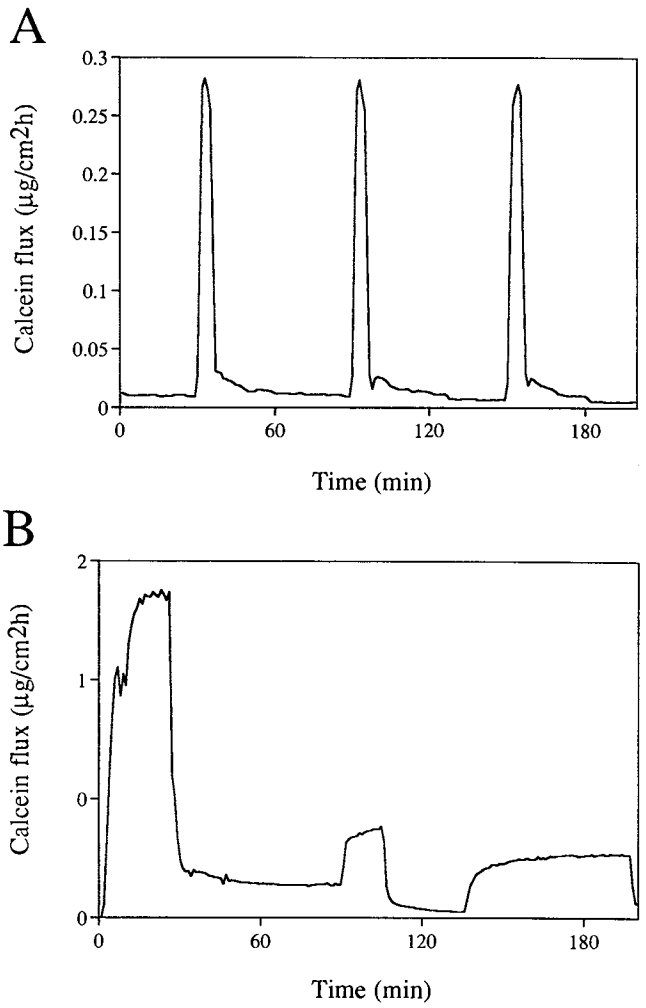

Fig. 2. Complex delivery profiles using transdermal delivery by electroporation. A) Continuous low-level delivery with intermittent boluses. Low-level delivery corresponded to continuous dc iontophoresis at 14 $\mu A/cm^2$. Boluses corresponded to pulsing at 115 V and 12 ppm for 5 min, each separated by 55 min of iontophoresis. The data in this figure are representative of results seen in 15 similar experiments. B) A complex delivery schedule achieved by changing pulse voltage. Pulse rate was held constant at 1 ppm, while pulse voltage was changed in the following sequence: 270 V for 30 min, 115 V for 60 min, 165 V for 15 min, 0 V for 30 min, 135 V for 60 min, 0 V for 5 min.

the time required to give 4 pulses, which determined the value for k_3.

The form of these flux equations does not yet have a mechanistic basis. Instead, their form was suggested by (a) the shape of the curves (see Fig. 1), which appear to approach a steady-state value exponentially, after an onset time (eq. 1), and (b) the observation that steady-state flux appeared to be proportional to pulse rate and voltage (eq. 2), while lag time (eq. 3) and onset time (eq. 4) appeared to be inversely proportional to pulse rate (see Table I).

The flux equations can predict the time profile of transdermal flux for a given pulse rate and voltage. Similarly, pulsing parameters can be determined for a desired delivery schedule. However, these equations are only valid under the conditions of this study and only over a limited range of electrical parameters. Given the large variability in flux across different skin samples from different donors, these equations should only be used in their present form for order of magnitude estimates.

Figures 2 and 3 show how the rapidly responsive behavior of transdermal drug delivery by electroporation can be used to achieve desired delivery profiles. For example, continuous low-level delivery of a drug with intermittent boluses may be a desirable delivery schedule for some drugs. To achieve this type of delivery, iontophoresis was applied to supply baseline delivery, while electroporation pulses provided rapid boluses (Figure 2A). A more complex delivery profile is shown in Figure 2B. In these figures, changes in delivery rates were achieved by changing pulse voltage. However, changes in pulse rate can also achieve similar results (data not shown).

Using the time-invariant pulsing protocols shown above, steady-state transport was achieved within minutes, depending on pulse rate used (e.g., Table I). However, we wanted to determine whether steady state could be reached more quickly by further improving the pulsing protocol. For this reason, an initial series of three pulses were applied

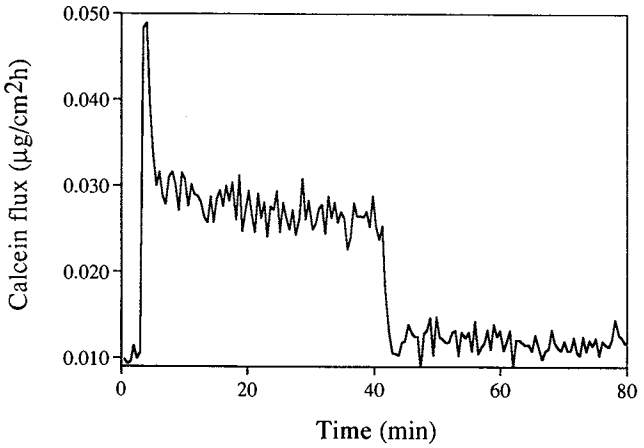

Fig. 3. More rapid attainment of steady-state flux using a time-varying pulse protocol. Reaching steady state within approximately 1 min, transdermal flux is shown due to pulsing at 165 V initially at 12 ppm (15 s) to "prime the pump," followed by pulsing at 1 ppm (40 min) to maintain the desired steady-state flux. The data in this figure are representative of results seen in 5 similar experiments.

more rapidly (12 ppm), to "prime the pump," followed by less rapid pulsing (1 ppm) to provide the desired steady-state flux. The result is shown in Figure 3, where steady state was achieved within approximately 1 min.

DISCUSSION

It has been previously demonstrated that electroporation of skin can cause reversible transdermal flux increases up to four orders of magnitude, which appear to involve transient structural changes within the stratum corneum (5,12). The present study shows that during skin electroporation, steady-state lag times and onset times of minutes can be achieved, indicating rapid temporal control of transport. In contrast, steady-state lag times associated with other methods of transdermal transport are often hours to days (1,2).

Flux versus time profiles were characterized by a simple set of empirical equations, which could be used to (a) predict delivery profiles under a given set of electroporation conditions and (b) select the pulsing conditions required to achieve a desired delivery schedule. While these equations have been determined only with limited data, additional characterization could yield equations which are more broadly applicable.

Examples of how specialized delivery profiles can be created using the rapid temporal control of electroporation are shown in Figures 2 and 3. Sequential application of different sets of pulsing conditions allowed creation of complex delivery profiles, limited by temporal control not faster than minutes. Better understanding of skin electroporation and further optimization of pulsing protocols may lead to still more rapid control of transport.

Many unresolved issues must be addressed before transdermal drug delivery by electroporation finds clinical application. However, an ability to increase transdermal transport by orders of magnitude with lag times of only minutes may be significant. Rapid onset of therapeutic action and/or complex drug delivery profiles could be achieved, where delivery rates could be swiftly adjusted by medical personnel, patients, or a microprocessor either (a) controlled by preprogrammed schedules or (b) interfaced with sensors for automatic feedback.

ACKNOWLEDGMENTS

We thank C. H. Liu, T. P. Singh, and V. G. Bose for technical assistance and helpful discussions. This work was supported in part by Cygnus Therapeutic Systems (MRP, JCW), the German Research Society (UP), Army Research Office Grant DAAL03-90-G-0218 (JCW), and National Institutes of Health Grants GM44884 (RL) and GM34077 (JCW).

REFERENCES

1. R. L. Bronaugh and H. I. Maibach (eds). *Percutaneous Absorption, Mechanisms—Methodology—Drug Delivery*. Marcel Dekker, New York, 1989.
2. J. Hadgraft and R. H. Guy (eds). *Transdermal Drug Delivery: Developmental Issues and Research Initiatives*. Marcel Dekker, New York, 1989.
3. M. R. Prausnitz, V. G. Bose, R. Langer, and J. C. Weaver. Transdermal drug delivery by electroporation. *Proceed. Intern. Symp. Control. Rel. Bioact. Mater.* 19:232–233 (1992).
4. D. Bommannan, L. Leung, J. Tamada, J. Sharifi, W. Abraham, and R. Potts. Transdermal delivery of luteinizing hormone releasing hormone: comparison between electroporation and iontophoresis in vitro. *Proceed. Intern. Symp. Control. Rel. Bioact. Mater.* 20:97–98 (1993).
5. M. R. Prausnitz, V. G. Bose, R. Langer, and J. C. Weaver. Electroporation of mammalian skin: a mechanism to enhance transdermal drug delivery. *Proc. Natl. Acad. Sci. USA.* 90:10504–10508 (1993).
6. V. G. Bose. *Electrical Characterization of Electroporation of Human Stratum Corneum*. MS Thesis, Massachusetts Institute of Technology, Cambridge, MA, 1994.
7. M. R. Prausnitz, D. S. Seddick, A. A. Kon, V. G. Bose, S. Frankenburg, S. N. Klaus, R. Langer, and J. C. Weaver. Methods for in vivo tissue electroporation using surface electrodes. *Drug Delivery* 1:125–131 (1993).
8. E. Neumann, A. E. Sowers, and C. A. Jordan, eds. *Electroporation and Electrofusion in Cell Biology*. Plenum Press, New York, 1989.
9. D. C. Chang, B. M. Chassy, J. A. Saunders, and A. E. Sowers, eds. *Guide to Electroporation and Electrofusion*. Academic Press, New York, 1992.
10. S. Orlowski and L. M. Mir. Cell electropermeabilization: a new tool for biochemical and pharmacological studies. *Biochim. Biophys. Acta.* 1154:51–63 (1993).
11. J. C. Weaver. Electroporation: a general phenomenon for manipulating cells and tissues. *J. Cell. Biochem.* 51:426–435 (1993).
12. M. R. Prausnitz, V. G. Bose, R. Langer, and J. C. Weaver. Electroporation. In H. I. Maibach and E. W. Smith (eds.), *Percutaneous Penetration Enhancers*, CRC Press, Boca Raton, FL, in press.
13. U. Pliquett, M. R. Prausnitz, Y. A. Chizmadzhev, and J. C. Weaver. Measurement of rapid release kinetics for transdermal and other types of drug delivery (submitted).
14. U. Pliquett, R. Langer, and J. C. Weaver. The change in the passive electrical properties of human stratum corneum due to electroporation (submitted).